CORE
Metadata, citation and similar papers at core.ac.uk
Provided by Online Research Database In Technology

Technical University of Denmark

Constitutional and thermal point defects in B2 NiAl

Korzhavyi, P. A.; Ruban, Andrei; Lozovoi, A. Y.; Vekilov, Yu. Kh.; Abrikosov, I. A.; Johansson, B.

Published in:
Physical Review B (Condensed Matter and Materials Physics)

Link to article, DOI:
10.1103/PhysRevB.61.6003

Publication date:
2000

Document Version
Publisher's PDF, also known as Version of record

Link back to DTU Orbit

Citation (APA):
Korzhavyi, P. A., Ruban, A., Lozovoi, A. Y., Vekilov, Y. K., Abrikosov, I. A., & Johansson, B. (2000). Constitutional and thermal point defects in B2 NiAl. Physical Review B (Condensed Matter and Materials Physics), 61(9), 6003-6018. DOI: 10.1103/PhysRevB.61.6003

DTU Library
Technical Information Center of Denmark

General rights
Copyright and moral rights for the publications made accessible in the public portal are retained by the authors and/or other copyright owners and it is a condition of accessing publications that users recognise and abide by the legal requirements associated with these rights.

- Users may download and print one copy of any publication from the public portal for the purpose of private study or research.
- You may not further distribute the material or use it for any profit-making activity or commercial gain
- You may freely distribute the URL identifying the publication in the public portal

If you believe that this document breaches copyright please contact us providing details, and we will remove access to the work immediately and investigate your claim.

Constitutional and thermal point defects in *B*2 NiAl

P. A. Korzhavyi
Condensed Matter Theory Group, Department of Physics, Uppsala University, S-75121 Uppsala, Sweden

A. V. Ruban
Center for Atomic-Scale Materials Physics and Department of Physics, Technical University of Denmark, DK-2800 Lyngby, Denmark

A. Y. Lozovoi
Atomistic Simulation Group, School of Mathematics and Physics, The Queen's University of Belfast, Belfast BT7 1NN, United Kingdom

Yu. Kh. Vekilov
Department of Theoretical Physics, Moscow Institute of Steel and Alloys, 4, Leninskiy prospect, 117936 Moscow, Russia

I. A. Abrikosov and B. Johansson
Condensed Matter Theory Group, Department of Physics, Uppsala University, S-75121 Uppsala, Sweden
(Received 15 July 1999)

The formation energies of point defects and the interaction energies of various defect pairs in NiAl are calculated from first principles within an order *N*, locally self-consistent Green's-function method in conjunction with multipole electrostatic corrections to the atomic sphere approximation. The theory correctly reproduces the ground state for the off-stoichiometric NiAl alloys. The constitutional defects (antisite Ni atoms and Ni vacancies in Ni-rich and Al-rich NiAl, respectively) are shown to form ordered structures in the ground state, in which they tend to avoid each other at the shortest distance on their sublattice. The dominant thermal defects in Ni-rich and stoichiometric NiAl are calculated to be triple defects. In Al-rich alloys another type of thermal defect dominates, where two Ni vacancies are replaced by one antisite Al atom. As a result, the vacancy concentration decreases with temperature in this region. The effective defect formation enthalpies for different concentration regions of NiAl are also obtained.

I. INTRODUCTION

The outstanding physical, chemical, and mechanical properties of the intermetallic compound NiAl (Refs. 1,2) have given rise to a variety of commercial applications in the aircraft industry, electronics, and catalysis industry. During the last decade, a number of *ab initio* studies of NiAl have been performed in order to describe the nature of the interatomic bonding,[3–6] electronic structure,[7–12] cohesive properties,[7,13–17] defect energetics,[18–22] and optical properties[23–27] of this Hume-Rothery electronic compound leading to a scientific basis for the understanding of the complicated phenomena which take place during manufacturing and application of NiAl-containing alloys.

The structure of point defects in NiAl has been the subject of experimental and theoretical studies since the pioneering work of Bradley and Taylor[28] (see also Ref. 29) who have shown that the variation of the lattice parameter and weight density of NiAl with alloy composition can be successfully explained only if one assumes that antisite Ni atoms on the Al sublattice exist in the Ni-rich off-stoichiometric NiAl-based alloys, while the deviation from the exact stoichiometry in the Al-rich alloys is formed due to vacancies on the Ni sublattice.

The existence of constitutional vacancies in NiAl was initially understood as a tendency of the alloy to keep the number of valence electrons per unit cell below a certain limit ($3e$/cell) in order to prevent filling the energetically unfavorable electronic states in the next Brillouin zone. This kind of explanation is applicable to some alloys and compounds with predominantly metallic chemical bonding.[30–32] Since the covalent and ionic components of the interatomic bonding are rather strong in NiAl,[5] the explanation in terms of electron concentration does not seem to be entirely convincing. Moreover, the electron concentration has been found to exceed the limit of $3\,e$/cell in ternary Ni-Al-Cu B2-based alloys,[33] where it may reach a value as high as $3.38\,e$/cell. Recent studies performed by Smirnov[34,35] and by Cottrell[36,37] show that the stability and even the ordering of constitutional vacancies may be satisfactorily explained in terms of local bond strengths, which is consistent with the local nature of the chemical bonding in NiAl. Within the local bond picture, the tendency of NiAl to form constitutional vacancies on the Al-rich side may be attributed to the fact that the Al-Al bond is much weaker than the Ni-Ni or Al-Ni bonds.

However, Fermi-surface effects may still play a significant role in the off-stoichiometric Ni-rich NiAl. It has been first shown by Egorushkin *et al.*[38] and later by Zhao and Harmon[39] and Stocks *et al.*,[40] that a distinct nesting feature of the Fermi surface of $Ni_{0.625}Al_{0.375}$ may be related to the 7R fcc-based structure of NiAl Martensite. The competition in energy between the bcc- and fcc-based structures of Ni-Al alloys which takes place in the interval 50–75 at. % Ni (Refs. 13,15) explains why the system is so sensitive to the details of the Fermi surface in this compositional region.

Crystal structures suggested for the NiAl Martensite[41–43]

 ©2000 The American Physical Society

may require a certain type of ordering of antisite defects in the Ni-rich NiAl. Short-range ordering of the constitutional vacancies in the Al-rich NiAl is also expected from experiment.[44–46] The crystal structures of the phases adjacent to NiAl: Ni_2Al_3,[28,29] Ni_3Al_4,[47] and Ni_5Al_3 (Ref. 48) may be considered as ordered structures of constitutional defects on the $B2$ underlying lattice. Thus, the defect ordering is important for understanding the structural transformations in NiAl.

The thermal disorder in NiAl is also unusual. Thermal defects in an ordered binary alloy of a fixed composition must appear in a balanced manner in order to preserve the alloy stoichiometry. For example, an elementary thermal defect in Ni_3Al may be described as an exchange of pairs of antisite (Al and Ni) atoms.[49] Thermal disorder in the $B2$-type intermetallics is often of a triple defect type[50] and the triple defect formed by two Ni vacancies and one antisite Ni atom is considered to be the dominant thermal excitation in NiAl.[1,2]

The equilibrium concentrations of thermal defects in NiAl have been investigated by means of semiempirical models[51,34,35,52] as well as on the basis of first-principles calculations[18,19,22] and atomic-scale simulations.[53–55] The considerations are commonly based on the model of a gas of noninteracting point defects as proposed by Wagner and Schottky.[56] This model has been used to study defects in intermetallics using either a canonical[54,55] or grand canonical[18,22,57–59] formalism. The two formalisms are equivalent[60] in the sense that they must yield the same results for the equilibrium defect concentrations. However, the canonical formalism is more conveniently applied to the case of a single-phase alloy at a fixed atomic composition, where it allows for a simple theoretical description of thermal defects, as will be shown in Secs. II and V.

First-principles calculations by Fu *et al.*[18] have confirmed that in stoichiometric as well as in Ni-rich NiAl the dominant thermal excitations are indeed of the triple defect type. However, for the Al-rich compositions, a relatively high concentration of antisite Al atoms on the Ni sublattice is obtained numerically[18] and also expected from x-ray diffraction experiments.[61] The calculated equilibrium concentration of the antisite Ni atoms in the Al-rich NiAl is unexpectedly low.[18] Furthermore, using a semiempirical mean-field approach, Smirnov[34,35] has shown that one can expect an anomalous thermal behavior of the equilibrium vacancy concentration for the Al-rich compositions where the temperature dependence of the vacancy concentration may have a minimum. All this clearly shows that the actual statistics of thermal defects in Al-rich NiAl is inconsistent with the triple defect model.

In this work we perform *ab initio* calculations of the electronic structure and total energy of NiAl intermetallic compounds containing four types of point defects (two vacancies and two antisite defects) in different combinations and spatial configurations in order to find the defect formation enthalpies and pair defect interaction energies. Based on the obtained values, we study the type of constitutional defects as well as the statistics of thermal defects. We show that the statistics of thermal defects can be interpreted in terms of composition-conserving defects and that in the Al-rich region at low temperatures the dominant thermal defect is of a different, so-called interbranch type. A simplified analytical treatment of thermal defects is proposed for the nearly stoichiometric as well as for the concentrated off-stoichiometric NiAl alloys. The obtained analytical expressions allow for a physically transparent interpretation of the effective defect formation energies and volumes as well as their concentration dependencies.

II. GENERAL FORMALISM

A. Alloy configurations

We will consider a single-phase $B2$ NiAl alloy having a fixed atomic composition, $Ni_{1/2-\delta}Al_{1/2+\delta}$, where δ is the deviation from stoichiometry. The alloy components (Al and Ni atoms) and vacancies, $i=\{\mathrm{Al,Ni},V\}$, occupy N lattice sites on the two sublattices ($\alpha=\{\mathrm{Al,Ni}\}$) of the $B2$ structure. Each sublattice has $N_\alpha=\frac{1}{2}N$ sites occupied by n_{i_α} atoms or vacancies.

In the canonical ensemble the number of Al atoms $n_{\mathrm{Al}}=n_{\mathrm{Al_{Al}}}+n_{\mathrm{Al_{Ni}}}$ and the number of Ni atoms $n_{\mathrm{Ni}}=n_{\mathrm{Ni_{Al}}}+n_{\mathrm{Ni_{Ni}}}$ are fixed. At the same time, the number of vacancies in the alloy $n_V=n_{V_{\mathrm{Al}}}+n_{V_{\mathrm{Ni}}}$ as well as the total number of lattice sites N may vary. The distribution of alloy components between the sublattices may be described in terms of *site* concentrations: $c_{i_\alpha}=n_{i_\alpha}/N_\alpha$. However, since the number of lattice sites is not conserved in the presence of vacancies, it is more convenient to use *atomic* concentrations defined with respect to the total number of atoms $N_{at}=n_{\mathrm{Al}}+n_{\mathrm{Ni}}$:

$$x_{i_\alpha}=\frac{n_{i_\alpha}}{N_{at}}. \tag{1}$$

If necessary, one can easily transform between the atomic and site concentrations using the following relationship: $c_{i_\alpha}=2x_{i_\alpha}/(1+x_V)$, where $x_V=n_V/N_{at}$ is the net concentration of vacancies.

With these definitions, one has six atomic concentrations and three constraints

$$\sum_i x_{i_{\mathrm{Al}}}=\sum_i x_{i_{\mathrm{Ni}}},$$

$$x_{\mathrm{Al}}=\sum_\alpha x_{\mathrm{Al}_\alpha}=\frac{1}{2}+\delta,$$

$$x_{\mathrm{Ni}}=\sum_\alpha x_{\mathrm{Ni}_\alpha}=\frac{1}{2}-\delta, \tag{2}$$

which reflects the fact that the numbers of lattice sites on the two sublattices are equal and that the numbers of Al and Ni atoms are conserved.

The problem is to find four concentrations, x_d, of point defects: two antisite atoms, $d=\{\mathrm{Ni_{Al}},\mathrm{Al_{Ni}}\}$, and two vacancies, $d=\{V_{\mathrm{Al}},V_{\mathrm{Ni}}\}$, as a function of temperature T, pressure p, and deviation from stoichiometry δ. According to Eq. (2), only three of the four defect concentrations are independent:

$$x_{\mathrm{Al_{Ni}}}-x_{\mathrm{Ni_{Al}}}+\frac{1}{2}(x_{V_{\mathrm{Ni}}}-x_{V_{\mathrm{Al}}})=\delta. \tag{3}$$

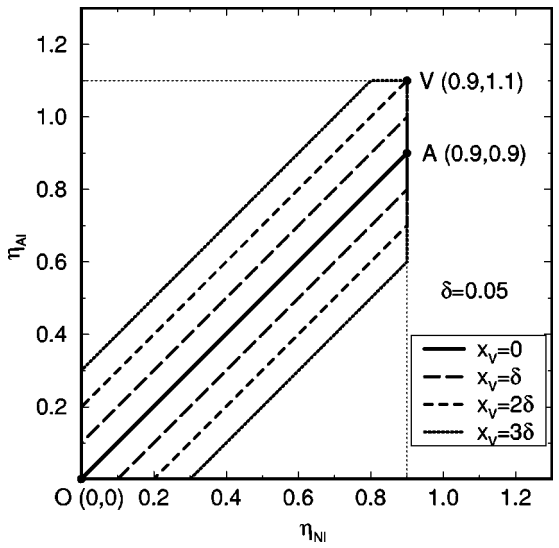

FIG. 1. Three-dimensional domain of possible configurations for the binary off-stoichiometric $Ni_{0.45}Al_{0.55}$ alloy. The boundary of the domain is shown by contour lines in the $\eta_{Ni}-\eta_{Al}$ plane for different vacancy concentrations x_V. Point O corresponds to a completely disordered state of the alloy with no vacancies. Points *A* or *V* correspond to maximally ordered states of the alloy having antisite atoms or vacancies, respectively, as constitutional defects.

Alternatively, the atomic order can be specified by three other independent variables: the net concentration of vacancies and two long-range order (LRO) parameters[62]

$$x_V = x_{V_{Ni}} + x_{V_{Al}},$$

$$\eta_{Ni} = 2(x_{Ni_{Ni}} - x_{Ni_{Al}}),$$

$$\eta_{Al} = 2(x_{Al_{Al}} - x_{Al_{Ni}}). \tag{4}$$

The atomic concentrations of the alloy components can be uniquely expressed through these three variables as follows:

$$4x_{Al_{Al}} = 2x_{Al} + \eta_{Al}, \quad 4x_{Al_{Ni}} = 2x_{Al} - \eta_{Al},$$

$$4x_{Ni_{Al}} = 2x_{Ni} - \eta_{Ni}, \quad 4x_{Ni_{Ni}} = 2x_{Ni} + \eta_{Ni},$$

$$4x_{V_{Al}} = 2x_V - \eta_{Al} + \eta_{Ni}, \quad 4x_{V_{Ni}} = 2x_V + \eta_{Al} - \eta_{Ni}. \tag{5}$$

In Fig. 1 we show the domain of possible configurations for the alloy $Ni_{0.45}Al_{0.55}$ as a contour plot in the (η_{Al}, η_{Ni}) plane for different vacancy concentrations. At zero vacancy concentration, the configurational space of the LRO parameters is restricted to the segment $|OA|$. For a nonzero vacancy concentration, the configurational space expands to a band of finite width which is restricted by the natural bounds of the LRO parameters $|\eta_{Al}| \leq 1+2\delta$ and $|\eta_{Ni}| \leq 1-2\delta$.

Infinitesimal changes of the variables x_V, η_{Ni}, and η_{Al} correspond to the following three processes, respectively: a divacancy formation (D), a jump of a vacancy from the Al to the Ni sublattice with a simultaneous formation of a Ni antisite defect on the Al sublattice (*JN*), and a jump of a vacancy from the Ni to the Al sublattice with the simultaneous formation of an Al antisite defect on the Ni sublattice (*JA*). These processes can be expressed in the form of defect reactions:

$$0 \rightarrow V_{Ni} + V_{Al},$$

$$V_{Al} \rightarrow V_{Ni} + Ni_{Al},$$

$$V_{Ni} \rightarrow V_{Al} + Al_{Ni}, \tag{6}$$

respectively. Hereafter we follow the quasichemical convention and omit the Al_{Al} and Ni_{Ni} in the equations of defect reactions.

B. Wagner-Schottky model

The equilibrium state of the alloy at temperature T and pressure p is determined by the minimum of the Gibbs free energy G or, equivalently, of its excess value ΔG defined relative to some standard states and normalized *per atom*:

$$\Delta G = \Delta E + p\Delta\Omega - T\Delta S. \tag{7}$$

Here ΔE, $\Delta\Omega$, and ΔS are the alloy formation energy, volume and entropy, respectively. As the standard states we choose here pure fcc Ni and Al and, therefore, the energy of alloy formation is defined as

$$\Delta E = E_{Ni_{1/2-\delta}Al_{1/2+\delta}} - x_{Ni}E_{Ni} - x_{Al}E_{Al}, \tag{8}$$

which, combined with the second term in Eq. (7), gives the enthalpy (or heat) of alloy formation ΔH:

$$\Delta H = \Delta E + p\Delta\Omega. \tag{9}$$

It is well known that the enthalpy of alloy formation[63] and the lattice parameter[28,29] of NiAl are essentially linear functions of the alloy composition. In such a case the Wagner-Schottky model[56] exploiting the picture of a gas of noninteracting point defects on well-defined sublattices may be applied. The model rests on two basic assumptions.

(i) The enthalpy of alloy formation depends linearly on the defect concentrations,

$$\Delta H = \Delta H_{NiAl} + \sum_d H_d x_d, \tag{10}$$

where ΔH_{NiAl} is the enthalpy of formation of the stoichiometric NiAl and H_d is the defect formation enthalpy.

(ii) Only the mean-field configurational entropy is taken into account,

$$S = (1+x_V)\ln\left(\frac{1+x_V}{2}\right) - \sum_\alpha \sum_i x_{i_\alpha} \ln x_{i_\alpha}, \tag{11}$$

where $i=\{Al, Ni, V\}$ and $\alpha=\{Al, Ni\}$. The parameters of the Wagner-Schottky model are the defect formation enthalpies

$$H_d = \frac{\partial \Delta H}{\partial x_d}. \tag{12}$$

In practice, it is common to linearize the pressure dependence of the defect formation enthalpy at $p=0$, i.e.,

$$H_d = E_d + p\Omega_d, \tag{13}$$

where E_d is the defect formation energy and Ω_d is the defect formation volume which may be obtained from the results of *ab initio* calculations performed at $T=0$ and $p=0$:

$$E_d=\frac{\partial \Delta E}{\partial x_d}, \quad \Omega_d=\frac{\partial \Delta \Omega}{\partial x_d}. \tag{14}$$

The minimization of the Gibbs excess free energy in configurational space $(x_V, \eta_{\mathrm{Ni}}, \eta_{\mathrm{Al}})$ in the Wagner-Schottky model leads to the following set of Bragg-Williams-type equations for equilibrium defect concentrations:

$$\frac{4x_{V_{\mathrm{Al}}}x_{V_{\mathrm{Ni}}}}{(1+x_V)^2}=\exp[-H_D/T], \tag{15a}$$

$$\frac{x_{\mathrm{Ni}_{\mathrm{Al}}}x_{V_{\mathrm{Ni}}}}{x_{\mathrm{Ni}_{\mathrm{Ni}}}x_{V_{\mathrm{Al}}}}=\exp[-H_{JN}/T], \tag{15b}$$

$$\frac{x_{\mathrm{Al}_{\mathrm{Ni}}}x_{V_{\mathrm{Al}}}}{x_{\mathrm{Al}_{\mathrm{Al}}}x_{V_{\mathrm{Ni}}}}=\exp[-H_{JA}/T]. \tag{15c}$$

Here H_D, H_{JA}, and H_{JN} are the enthalpies of the defect reactions (6) which are connected with the formation enthalpies of the four point defects by the following equations:

$$H_D=H_{V_{\mathrm{Al}}}+H_{V_{\mathrm{Ni}}},$$

$$H_{JN}=H_{\mathrm{Ni}_{\mathrm{Al}}}+H_{V_{\mathrm{Ni}}}-H_{V_{\mathrm{Al}}},$$

$$H_{JA}=H_{\mathrm{Al}_{\mathrm{Ni}}}+H_{V_{\mathrm{Al}}}-H_{V_{\mathrm{Ni}}}. \tag{16}$$

Expressed in terms of the site concentrations, the set of equations (15) take the usual form of mass action law for the quasichemical reactions (6). The equilibrium defect concentrations can be found either numerically by solving Eq. (15) together with Eq. (3), as is done in the present work, or even analytically by a reduction to fourth-order polynomial equations for the site concentrations as shown by Hagen and Finnis.[55]

C. Constitutional defects in off-stoichiometric alloys

The *ground state* structure of an alloy is that which minimizes its free energy or, equivalently, the formation enthalpy at $T=0$. According to the Nernst theorem the ground state of a binary off-stoichiometric alloy must be either a fully ordered phase or a mixture of two ordered phases. However, if one deals with an alloy such as NiAl, which is stable in a wide single-phase region, it is convenient to consider its *maximally ordered state*[49] which is the ground state of the alloy under the restriction that the alloy does not undergo a phase separation. It is obvious from Eq. (3) that in the maximally ordered state of an off-stoichiometric alloy ($\delta \neq 0$) there should be a finite concentration of either antisite atoms or vacancies on the sublattice of the deficient alloy component. The defects which are actually present in the maximally ordered state are called *constitutional defects*.

Although in general both antisite defects and vacancies may be present in the maximally ordered state, the defect of only one type is usually stable in the off-stoichiometric alloy at 0 K, which is also the case of NiAl. This is also consistent with the Wagner-Schottky model in which the enthalpy of alloy formation is a linear function of defect concentrations and thus the presence of two kinds of defects in the maximally ordered state is an exception.

In the configurational space of the LRO parameters $(\eta_{\mathrm{Al}}, \eta_{\mathrm{Ni}})$, the maximally ordered state corresponds to one of the vertexes of the domain of possible alloy configurations. For instance, the maximally ordered state of the $Ni_{0.45}Al_{0.55}$ off-stoichiometric alloy presented in Fig. 1 should be either at vertex *A* if the constitutional defects are antisite Al atoms or at vertex *V* if the constitutional defects are Ni vacancies.

The stability of antisite defects relative to vacancies is determined by their enthalpies of formation, Eq. (12), or, in other words, by the slopes of the two *branches* of the enthalpy of alloy formation $\Delta H(\delta)$ considered as a function of concentration of either vacancies or antisite defects. From Eq. (3) one finds that the concentration of constitutional defects is $x^c_{A_\alpha}=|\delta|$ in the case of antisites or $x^c_{V_\alpha}=2|\delta|$ in the case of vacancies (the superscript *c* stands for the constitutional defects). Therefore, a necessary condition for vacancies to become the constitutional defects in off-stoichiometric alloys is $2H_{V_{\mathrm{Ni}}}<H_{\mathrm{Al}_{\mathrm{Ni}}}$ for the Al-rich region and $2H_{V_{\mathrm{Al}}}<H_{\mathrm{Ni}_{\mathrm{Al}}}$ for the Ni-rich region.

D. Thermal defects

The *thermal defects* appear at a finite temperature in addition to the constitutional defects. Since the alloy composition is fixed they can appear only in the composition-conserving combination of single point defects obeying the condition

$$x^t_{\mathrm{Al}_{\mathrm{Ni}}}-x^t_{\mathrm{Ni}_{\mathrm{Al}}}+\frac{1}{2}(x^t_{V_{\mathrm{Ni}}}-x^t_{V_{\mathrm{Al}}})=0 \tag{17}$$

so that the total defect concentrations $x_d=x^c_d+x^t_d$, again satisfy Eq. (3).

It follows from Eq. (17) that none of the point defects can be a thermal defect alone. Point defects may be thermally generated at least in pairs or in some other possible combination, i.e., as a *composition-conserving defect* (CD). In general, a thermal defect may consist of several point defects with a specific spatial arrangement due to the interactions of the point defects with each other and also with the constitutional defects. It is obvious, however, that if the point defect interactions are relatively weak, the thermal defects will appear as the simplest composition-conserving combinations of points defects, provided that, in the most common situation, one thermal defect is dominant over the others.[64]

Which thermal defect is the dominant one, can be determined from the equilibrium concentrations of individual point defects x^t_d by comparing their relative ratio to that of the composition-conserving defects. The simplest composition-conserving defects are listed below for a general case of an arbitrary alloy composition and then, separately, for the off-stoichiometric alloys in which there is an additional degree of freedom due to the presence of the constitutional defects.

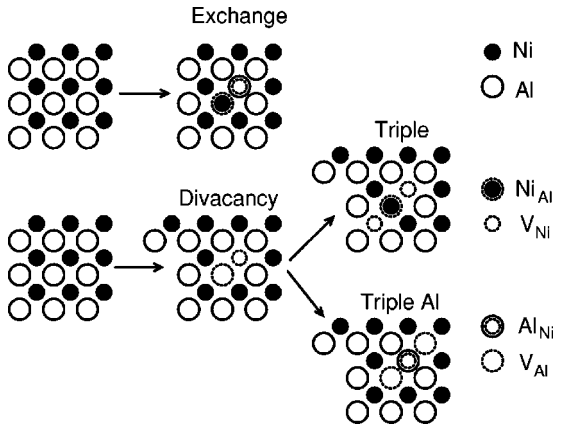

FIG. 2. Two-dimensional scheme illustrating some typical composition-conserving defects in $B2$ NiAl.

1. General case

There are four simplest composition-conserving defects consisting of two types of point defects[64] which can be thermally activated in the maximally ordered alloy of any composition including the defect-free stoichiometric alloy (the defects are schematically shown in Fig. 2). The defect reactions and the relations between the concentrations of thermal point defects are as follows.

Exchange antisite defect (X),

$$0 \rightarrow \mathrm{Ni_{Al}} + \mathrm{Al_{Ni}}: \quad x_X = x^t_{\mathrm{Ni_{Al}}} = x^t_{\mathrm{Al_{Ni}}}. \tag{18}$$

Divacancy or Schottky defect (D):

$$0 \rightarrow V_{\mathrm{Al}} + V_{\mathrm{Ni}}: \quad x_D = x^t_{V_{\mathrm{Al}}} = x^t_{V_{\mathrm{Ni}}}. \tag{19}$$

Triple Ni or simply triple defect (TN):

$$0 \rightarrow 2V_{\mathrm{Ni}} + \mathrm{Ni_{Al}}: \quad x_{\mathrm{TN}} = \frac{1}{2} x^t_{V_{\mathrm{Ni}}} = x^t_{\mathrm{Ni_{Al}}}. \tag{20}$$

Triple Al defect (TA):

$$0 \rightarrow 2V_{\mathrm{Al}} + \mathrm{Al_{Ni}}: \quad x_{\mathrm{TA}} = \frac{1}{2} x^t_{V_{\mathrm{Al}}} = x^t_{\mathrm{Al_{Ni}}}. \tag{21}$$

The formation enthalpy of a composition-conserving defect H_{CD} may be defined as the enthalpy of the corresponding quasichemical reaction. Thus, for the exchange, triple Ni, and triple Al defects one has

$$\begin{aligned} H_X &= H_{\mathrm{Ni_{Al}}} + H_{\mathrm{Al_{Ni}}} = H_{JN} + H_{JA}, \\ H_{\mathrm{TN}} &= H_{\mathrm{Ni_{Al}}} + 2H_{V_{\mathrm{Ni}}} = H_{JN} + H_D, \\ H_{\mathrm{TA}} &= H_{\mathrm{Al_{Ni}}} + 2H_{V_{\mathrm{Al}}} = H_{JA} + H_D, \end{aligned} \tag{22}$$

respectively, where we have also established the connection to the enthalpies (16) of defect reactions (6).

The pressure dependence of the formation enthalpy of a composition-conserving defect may also be represented in the form (13). The formation energy (volume) of the composition-conserving defect is then the sum of the formation energies (volumes) of its constituents.

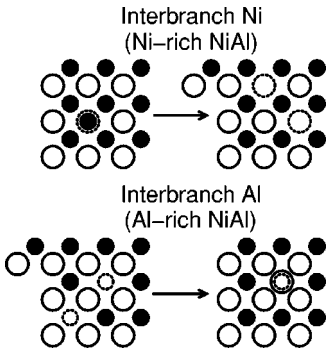

FIG. 3. Interbranch defects in Ni-rich and Al-rich NiAl. Note that interbranch defects are composition conserving.

2. Off-stoichiometric alloys

As mentioned above, the presence of the constitutional defects in the maximally ordered state of an off-stoichiometric alloy gives an additional possibility to satisfy Eq. (17) by replacing the constitutional antisites by vacancies and vice versa. In this case the concentration of the thermal point defects of the same type as the constitutional defects may take on a negative value.

Since the process of formation of such defects may be viewed as a transition of the alloy from the stable to the unstable branch, we will call it an *interbranch* defect. The formation of an interbranch defect is accompanied by the annihilation of the constitutional defects. Interbranch defects in NiAl are shown schematically in Fig. 3 for the Ni-rich region where the constitutional defects are Ni antisites and for the Al-rich region where the constitutional defects are Ni vacancies. The defect reactions and the concentrations of thermal point defects are as follows.

Interbranch Ni defect (IN):

$$\mathrm{Ni_{Al}} \rightarrow 2V_{\mathrm{Al}}: \quad x_{\mathrm{IN}} = -x^t_{\mathrm{Ni_{Al}}} = \frac{1}{2} x^t_{V_{\mathrm{Al}}}. \tag{23}$$

Interbranch Al defect (IA):

$$2V_{\mathrm{Ni}} \rightarrow \mathrm{Al_{Ni}}: \quad x_{\mathrm{IA}} = -x^t_{V_{\mathrm{Ni}}} = \frac{1}{2} x^t_{\mathrm{Al_{Ni}}}. \tag{24}$$

The formation enthalpies of the interbranch defects are

$$\begin{aligned} H_{\mathrm{IN}} &= 2H_{V_{\mathrm{Al}}} - H_{\mathrm{Ni_{Al}}} = H_D - H_{JN}, \\ H_{\mathrm{IA}} &= H_{\mathrm{Al_{Ni}}} - 2H_{V_{\mathrm{Ni}}} = H_{JA} - H_D. \end{aligned} \tag{25}$$

They characterize the relative stability of the antisite and vacancy branches in the Ni-rich and Al-rich NiAl, respectively. Since the antisite and vacancy branches in Al-rich $B2$ transition metal aluminides are competitive in energy, the interbranch Al defect may become the lowest-energy thermal defect in this compositional region.

E. Thermal defect concentrations: analytical consideration

In this section, simple analytical expressions for the concentrations of the main thermal defects in NiAl will be derived using the mass action law equations (15) and relations (22) and (25). Let us for now assume that a triple defect is

the dominant thermal defect in the stoichiometric NiAl, and that the defect concentrations in the maximally ordered state are

$$x^c_{\mathrm{Ni_{Al}}}=\begin{cases}-\delta, & \delta<0\\ 0, & \delta>0\end{cases},\quad x^c_{V_{\mathrm{Ni}}}=\begin{cases}0, & \delta<0\\ 2\delta, & \delta>0\end{cases}. \tag{26}$$

The validity of these assumptions is confirmed by the experimental data and by the first-principles calculations, as will be discussed in Secs. IV and V A. Since our analysis is performed in the framework of the Wagner-Schottky model, the results are valid only for noninteracting point defects.

1. Nearly stoichiometric NiAl

Nearly stoichiometric alloy is defined as an alloy in which the concentration of thermal defects is large compared to the concentration of constitutional defects, $|\delta|\ll x^t_d\ll 1$. The equilibrium concentration of triple defects in the stoichiometric NiAl ($\delta=0$) can be found using Eqs. (15a), (15b), and (20):

$$x_{\mathrm{TN}}\approx 2^{-5/3}\exp[-H_{\mathrm{TN}}/3T]. \tag{27}$$

The atomic concentrations of antisite Ni atoms and Ni vacancies are $x^t_{\mathrm{Ni_{Al}}}\approx x_{\mathrm{TN}}$ and $x^t_{V_{\mathrm{Ni}}}\approx 2x_{\mathrm{TN}}$.

The following expressions for the left-hand-side and right-hand-side first derivatives of x_{TN} with respect to δ can readily be obtained for nearly-stoichiometric NiAl:

$$\left.\frac{dx_{\mathrm{TN}}}{d\delta}\right|_{\delta=0}=\begin{cases}1/3, & \delta<0,\\ -2/3, & \delta>0.\end{cases} \tag{28}$$

It is noteworthy, that the first derivatives of the thermal defect concentrations are discontinuous at the stoichiometric composition, and independent of temperature. This discontinuity exactly compensates for the discontinuities in the first derivatives of the atomic concentrations of constitutional defects, Eq. (26). As a result, the total (constitutional plus thermal) defect concentrations, as well as the Gibbs free energy, are smooth functions of alloy composition in the vicinity of $\delta=0$ at finite temperatures.

2. Concentrated Ni-rich NiAl

Concentrated off-stoichiometric (Ni-rich or Al-rich) alloys are defined as alloys in which the concentration of constitutional defects is large compared to the concentration of thermal defects, $x^t_d\ll|\delta|\ll 1$. The estimate of the concentration of thermal triple defects in Ni-rich alloy ($\delta<0$) is

$$x_{\mathrm{TN}}\approx 2^{-5/2}(-\delta)^{-1/2}\exp[-H_{TN}/2T], \tag{29}$$

and the total atomic concentrations of point defects are $x_{\mathrm{Ni_{Al}}}\approx-\delta+x_{\mathrm{TN}}$ and $x_{V_{\mathrm{Ni}}}\approx 2x_{\mathrm{TN}}$.

3. Concentrated Al-rich NiAl

Considering triple defects as the dominant thermal defects in Al-rich NiAl ($\delta>0$), we find that their concentration decreases rapidly with increasing δ:

$$x_{\mathrm{TN}}\approx 2^{-5}\frac{1+2\delta}{\delta^2}\exp[-H_{\mathrm{TN}}/T]. \tag{30}$$

The atomic concentrations of point defects are $x_{\mathrm{Ni_{Al}}}\approx x_{\mathrm{TN}}$ and $x_{V_{\mathrm{Ni}}}\approx 2\delta+2x_{\mathrm{TN}}$.

On the other hand, if we assume that interbranch Al defects dominate, we arrive at

$$x_{\mathrm{IA}}\approx 2^3\frac{\delta^2}{1+2\delta}\exp[-H_{\mathrm{IA}}/T], \tag{31}$$

i.e., the concentration of defects grows almost quadratically with δ. The total atomic concentrations of point defects are $x_{V_{\mathrm{Ni}}}\approx 2\delta-2x_{\mathrm{IA}}$ and $x_{\mathrm{Al_{Ni}}}\approx x_{\mathrm{IA}}$. If the formation enthalpy of an interbranch Al defect is sufficiently small, one can expect a competition between triple and interbranch Al defects in the Al-rich NiAl.

F. Effective formation enthalpies

A subject that still remains confusing despite the fact that it has been addressed and clarified several times in the literature,[65,59,22] is the interpretation of the experimental data for so-called *effective* defect formation enthalpies in partially ordered alloys. The problem here originates from the unwarranted transfer of a simple formalism which is used to obtain the vacancy formation enthalpy in a monoatomic solid from the measured vacancy concentration, to the case of defects in partially ordered alloys.

The formalism is based on the Arrhenius formula connecting the equilibrium defect concentration with the effective defect formation enthalpy $H^{\mathrm{eff}}_d=E^{\mathrm{eff}}_d+p\Omega^{\mathrm{eff}}_d$ as follows:

$$c_d=\exp[-(H^{\mathrm{eff}}_d-TS^{\mathrm{eff}}_d)/T], \tag{32}$$

where S^{eff}_d is the effective defect formation entropy, associated with *nonconfigurational* effects during defect formation process. Except for its nonconfigurational part, this formula is a direct analog of Eq. (15a) in the case of a monoatomic solid. In a binary equiatomic compound, the equilibrium defect concentrations are solutions to the complete set of equations (3) and (15) and, therefore, the temperature dependencies of the defect concentrations are not expected to follow the Arrhenius form in general.

Let us first address the question of whether Eq. (32) is fulfilled by *composition-conserving defects*. The answer is as follows: the concentration of composition-conserving defects does exhibit a pseudo-Arrhenius temperature dependence as in Eqs. (27)–(31), provided that the formation enthalpies of composition-conserving defects are well separated on the energy scale. However, there are two principal differences between the pseudo-Arrhenius temperature dependence of the equilibrium defect concentrations in binary compounds and the Arrhenius form (32).

(i) The effective formation enthalpy of a composition-conserving defect $H^{\mathrm{eff}}_{\mathrm{CD}}$ which can be derived from Eqs. (27)–(31) as

$$H^{\mathrm{eff}}_{\mathrm{CD}}=-\left.\frac{d\ln x^t_{\mathrm{CD}}}{dT^{-1}}\right|_{p=\mathrm{const}}, \tag{33}$$

turns out to be different from the actual defect formation enthalpy H_{CD} by a factor for which the following rule can be established: The *effective* formation enthalpy of a

composition-conserving defect H_{CD}^{eff} is equal to the actual formation enthalpy of this defect H_{CD} divided by the number of point defects of a *new* type (with respect to the defect structure at zero temperature) created in the crystal by one composition-conserving defect.

Indeed, from the examples worked out in Sec. II E we find that the effective formation enthalpy of a triple defect is $H_{TN}^{eff}=H_{TN}/2$ in the Ni-rich NiAl where only two Ni vacancies are the new point defects. Stoichiometric NiAl is defect-free in the ground state, and all three constituents of a triple defect will be the new point defects in that case, so one has $H_{TN}^{eff}=H_{TN}/3$ at the stoichiometric composition. Only one new point defect will be generated in Al-rich NiAl by a triple or interbranch Al defect: an antisite Ni or Al atom, respectively. As a result, one has $H_{TN}^{eff}=H_{TN}$ and $H_{IA}^{eff}=H_{IA}$.

(ii) In contrast to the case of monoatomic solids, the effective defect formation entropy in binary compounds must contain a certain *configurational* part which can be derived from the concentration-dependent pre-exponential factors in Eqs. (27)–(31).

G. Single point defects

The analysis based on the Arrhenius formula Eq. (32) may become quite misleading if applied to single point defects in partially ordered alloys.[59,22] The reason is that single point defects, including vacancies, are not composition conserving. Under the experimental conditions, where the alloy composition is fixed, single point defects can appear or annihilate only in combinations with other point defects, i.e., as composition-conserving defects. Therefore, the formation enthalpies of composition-conserving defects are the only well-defined quantities within the canonical ensemble. The effective formation enthalpy of a single point defect is just a formal parameter satisfying Eq. (32), but it should not be interpreted as the enthalpy required to create this defect. The effective formation enthalpy of a single point defect must contain contributions from all the other point defects involved in the corresponding defect reaction.

Nevertheless, since in many cases the concentrations of single point defects have a pseudo-Arrhenius temperature dependence, the corresponding analysis remains a useful experimental tool of extracting information regarding point defect energetics in NiAl and other compounds.[66,67] We therefore now outline the connection between the effective formation enthalpies of single point defects and the enthalpies of formation of the composition-conserving defects.

Using Eq. (33) as a definition and applying it to the set of equations (15) one obtains a relationship equivalent to Eqs. (16) but now for the effective formation enthalpies of single point defects. This relationship may be expressed as follows: The *actual* formation enthalpy of a composition-conserving defect is equal to the sum of the *effective* formation enthalpies of its constituents. To establish the inverse relationships, one can consider Eqs. (16) as a set of equations in which the effective formation energies of single point defects are unknowns.

For instance, the dominant thermal defect in the stoichiometric composition is the triple Ni defect which involves two Ni vacancies and one antisite Ni atom ($2V_{Ni}+Ni_{Al}$). Thus the effective formation enthalpies of a Ni vacancy and an antisite Ni atom are equal to each other and to the effective formation enthalpy of a triple Ni defect in this region, i.e., $H_{V_{Ni}}^{eff}=H_{Ni_{Al}}^{eff}=H_{TN}/3$ as has been obtained in Sec. II F. The effective formation enthalpies of the two remaining point defects, antisite Al atom and Al vacancy, can now be found using Eqs. (16) and (22): $H_{Al_{Ni}}^{eff}=H_X^{eff}-H_{Ni_{Al}}^{eff}$ and $H_{V_{Al}}^{eff}=H_D^{eff}-H_{V_{Ni}}^{eff}$.

TABLE I. Effective formation enthalpies of single point defects in Ni-rich ($\delta<0$), stoichiometric ($\delta=0$), and Al-rich ($\delta>0$) NiAl expressed through the formation enthalpies of composition-conserving defects.

Defect	$\delta<0$	$\delta=0$	$\delta>0$
Ni_{Al}	0	$H_{TN}/3$	H_{TN}
V_{Al}	$H_{IN}/2$	$H_D-H_{TN}/3$	H_D
Al_{Ni}	H_X	$H_X-H_{TN}/3$	H_{IA}
V_{Ni}	$H_{TN}/2$	$H_{TN}/3$	0

In the case of concentrated off-stoichiometric alloys ($x_d^t \ll x_d^c$) the only way to satisfy Eq. (32) is to assign a zero value to the effective formation enthalpy of the constitutional defects, thereby neglecting any temperature variation of their concentration. The other effective formation enthalpies can then be found from Eqs. (16). The final results are summarized in Table I.

In fact, each of the obtained relationships explicitly specifies the quasichemical reaction which creates the given kind of single point defect in the given compositional region of NiAl, except for the constitutional defects for which $H^{eff}=0$. It is also worth mentioning that the obtained effective formation enthalpies are equivalent to ''true'' defect formation enthalpies introduced by Mishin and Farkas.[53]

III. METHOD OF CALCULATIONS

We use 54-site ($3\times3\times3$) cubic supercells to simulate isolated defects, and 108-site ($3\times3\times6$) supercells to evaluate the defect interactions. To perform large supercell calculations we take advantage of the order-N, locally self-consistent Green's function (LSGF) method introduced by Abrikosov *et al.*[68] The method has been successfully applied to study ordered, disordered, and partially ordered metallic alloys.[69]

The original implementation of the LSGF method[68] is based on the atomic sphere approximation (ASA). The calculations performed within the ASA usually overestimate the vacancy formation energy by as much as a factor of 2.[70–72] This large error arises as a result of an inadequate treatment of the electron charge depletion around the vacancy caused by the spherical averaging of the electron density over each atomic sphere, and would clearly invalidate the calculations. A possible solution is to go beyond the ASA for the charge density but keep the ASA for the potential. This so-called ASA+M approach, which is the first step towards the full charge density technique,[73] turns out to have sufficient accuracy for surface energy,[74] and vacancy formation energy[75] calculations.

The details of our total energy calculations are as follows. Each atom of the supercell together with its three coordina-

tion shells of atoms was considered self-consistently as a local interaction zone (LIZ) embedded in the multisublattice effective medium of the LSGF method, having the symmetry of the $B2$ crystal structure. The central on-site block $G_{LL'}^{RR}$ of the Korringa-Kohn-Rostocker (KKR) Green's function matrix calculated in the atomic sphere approximation (ASA) was used to construct the charge density in the atomic sphere at a site R of the supercell. The spherical components of the charge density were used to calculate the standard ASA total energy,[69] whereas the non-spherical components of the electron density integrated over the atomic spheres formed the multipole moments Q_L^R. The latter were used to calculate the multipole contributions to the Madelung potential and energy:

$$V_0^R = \frac{1}{S} \sum_{R',L'} M_{0,L'}^{R,R'} Q_{L'}^{R'} \tag{34}$$

and

$$E_M = \frac{1}{2S} \sum_{R,L} Q_L^R \sum_{R',L'} M_{L,L'}^{R,R'} Q_{L'}^{R'}, \tag{35}$$

respectively. Here L is a short-hand notation for the (l,m) quantum numbers, $M_{L,L'}^{R,R'}$ is the multipole Madelung matrix which is equivalent to the conventional (unscreened) LMTO structure constants for the entire supercell, and S is the Wigner-Seitz radius. We used equal Wigner-Seitz radii for the atomic and empty spheres. Our calculations were performed using two basis sets: with the angular momentum cutoff, $l_{\max}=2$ and 3. Correspondingly, the nonzero multipole charges up to $l=4$ and 6 were taken into account. The total energy was calculated in the framework of the local density approximation (LDA) as well as within the generalized gradient approximation (GGA), exploiting the Perdew, Burke, and Ernzerhof[76] form of the exchange and correlation potential. The core states of Al and Ni were recalculated at each self-consistency loop using the soft-core approximation.

In order to obtain the equation of state, the total energy calculations for the 54-site supercells as well as for pure Al, Ni, and NiAl were performed at six different volumes to cover the pressure range from -50 to 250 Kbar. The total energies were fitted by fourth-order polynomials. The energies and volumes corresponding to zero external pressure were used to calculate the defect formation energies and volumes according to Eq. (14). Therefore, the effect of global relaxation of the crystal volume was taken into account in our calculations whereas the effect of local relaxation around the defects was not considered.

The pair interaction energy $E_{A-B,n}^{\text{int}}$ between two defects A and B separated by a distance corresponding to the nth coordination shell radius was calculated using 108-site supercells as a difference in total energy of the supercell containing this defect pair $E_{A-B,n}^{\text{tot}}$ and of the supercell where these defects were separated by the largest possible distance $E_{A-B,\max}^{\text{tot}}$,

$$E_{A-B,n}^{\text{int}} = E_{A-B,n}^{\text{tot}} - E_{A-B,\max}^{\text{tot}}. \tag{36}$$

The defect interaction energies were determined at a fixed volume corresponding to the calculated equilibrium lattice parameter of the stoichiometric NiAl.

IV. DEFECTS AT ZERO TEMPERATURE

Before we discuss the results of our calculations for defects in NiAl it is useful to analyze how well the thermodynamic properties of the defect-free, stoichiometric NiAl are described within the LSGF ASA+M method. In Table II we compare our results for the equilibrium lattice parameter, heat of formation, bulk modulus, and its pressure derivative for B2 NiAl obtained using three sets of parameters with experimental data as well as with the results of previous *ab initio* calculations.

Because of the cubic symmetry of all the atomic positions in perfect B2 NiAl, the effect of the multipole corrections to the ASA is practically negligible in the absence of lattice defects. Therefore, our results obtained using three different sets of parameters show only the effect of the basis set and of the exchange-correlation potential. The results of our LDA calculations with the angular momentum cutoff $l_{\max}=2$ are very close to experiment. When the basis set is increased to $l_{\max}=3$, the agreement with experiment becomes worse, but we observe the well-known tendency of the LDA to underestimate the lattice constant and overestimate the bulk modulus and heat of formation. This LDA overbinding is lifted when the gradient corrections are taken into account. The overall agreement of our GGA results with experiment is excellent even though the former are obtained within the atomic sphere approximation. Therefore, we consider the GGA $l_{\max}=3$ results as the most reliable and containing a minimal number of approximations. In the following, unless explicitly specified, only the results obtained within the GGA $l_{\max}=3$ setup will be reported.

A. Defect formation energies and volumes

In Fig. 4(a) we show the formation energies of the perfect, stoichiometric $B2$ NiAl alloy and of four off-stoichiometric alloys simulated by 54-site supercells, each containing one of the four point defects per supercell. For a comparison, in Fig. 4(a) we also show the experimental data on the heat of formation of NiAl alloys at 1100 K obtained by Henig and Lukas[63] (HL) corrected for the standard state of Al as suggested in Ref. 17. The linear (as within the Wagner-Schottky model) dependencies of the alloy formation energy for the cases when the deviation from stoichiometry is formed by each of the four point defects in NiAl, are shown in Fig. 4(a). On either side away from the exact stoichiometric composition, one can see two branches of alloys: one corresponding to alloys having constitutional antisite defects (antisite branch), and the other corresponding to alloys containing constitutional vacancies (vacancy branch).

Figure 4(a) shows that the lower branch of the alloy formation energy for Ni-rich NiAl corresponds to constitutional antisite Ni atoms, but for Al-rich NiAl, the alloys containing constitutional Ni vacancies have lower energy of formation. The calculated alloy formation energy for the stable branches (solid lines) and the experimental heat of formation have

TABLE II. Ground-state properties of stoichiometric NiAl: equilibrium lattice parameter a_0, heat of formation ΔH, bulk modulus B, and the pressure derivative of the bulk modulus B'.

Method	Details	a_0 (Å)	ΔH (eV/atom)	B (Mbar)	B'
Experiment		2.887[a]	−0.75,[b] −0.68[c]	1.66,[d] 1.56[e]	4.0±0.5[e]
ASW[f]	LDA	2.86	−0.75	2.0	
FLAPW	LDA	2.84[g]	−0.82,[h] −0.68[i,j]	1.86±0.07[h]	4.2±0.5[h]
PP	LDA	2.837[k]		1.85[k]	
LMTO	LDA	2.85,[h] 2.86[l,m]	−0.83,[h] −0.79[l,m]		
LSGF[n]	LDA, $l_{max}=2$	2.87	−0.81	1.8	4.0
	LDA, $l_{max}=3$	2.81	−0.84	2.0	4.5
	GGA, $l_{max}=3$	2.87	−0.76	1.7	3.8

[a]X-ray diffraction, Ref. 29.
[b]Calorimetry, Ref. 63, standard states are fcc Ni and liquid Al.
[c]Calorimetry, Ref. 17, standard states are fcc Ni and fcc Al.
[d]From single crystal elastic constants, Ref. 77.
[e]From equation of state of polycrystalline NiAl, Ref. 78.
[f]Reference 7.
[g]Reference 16.
[h]Reference 14, standard states are bcc Ni and bcc Al.
[i]Reference 10.
[j]FLASTO LDA, Ref. 17.
[k]Reference 22.
[l]Reference 13.
[m]Reference 15.
[n]This work.

similar slopes for the Ni-rich and Al-rich sides, whereas the slopes of the unstable branches (dashed lines) differ substantially from experiment.

In Fig. 4(b) we compare our results for the lattice parameter of NiAl alloys with the results of x-ray diffraction experiments of Bradley and Taylor[28] (BT) and Taylor and Doyle[29] (TD). A similarity in slopes of the concentration dependencies of the lattice parameter is seen between the results of our calculations for the stable branches and experimental data.

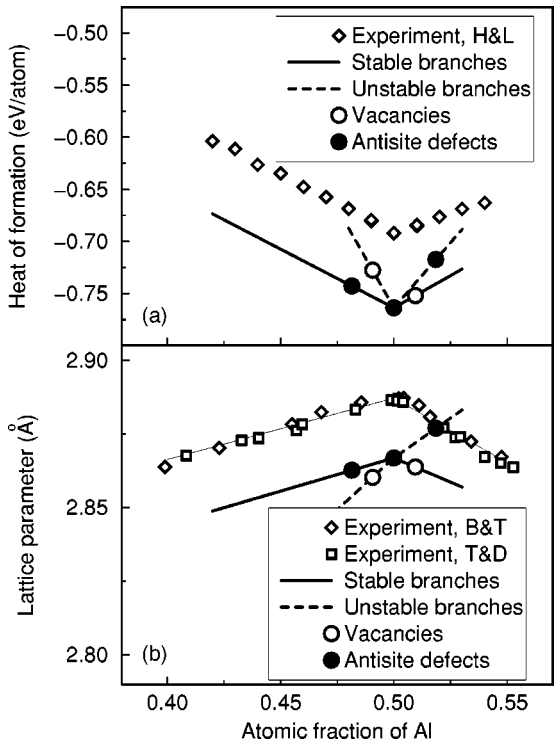

FIG. 4. Formation energy (a) and lattice parameter (b) of NiAl alloys as a function of alloy composition. Experimental data by Henig and Lukas (HL) (Ref. 63), Bradley and Taylor (BT) (Ref. 28), and Taylor and Doyle (TD) (Ref. 29) are shown for comparison.

The defect formation energies and volumes calculated using the three different sets of parameters are listed in Table III together with the estimates which are made from experimental concentration dependencies of the heat of formation[63] and lattice parameter.[28,29] The best overall agreement of the theoretical results and experimental estimates is obtained using the GGA $l_{max}=3$ setup which yields the lowest values of the defect formation energies. On the other hand, all the three sets of theoretical results qualitatively agree with each other and there is only a numerical difference in defect formation energies obtained using different sets of parameters.

Due to the fact that the formation energies of single point defects depend on the choice of the reference states, a direct comparison of our results given in Table III with the results of previous calculations, in which different reference states have been used, is not meaningful. On the other hand, the formation energies of composition-conserving defects, which do not depend on a particular choice of the reference states, can be compared directly. Thus we have used the data of Table III as well as the data reported in Refs. 18,22,53 to obtain the formation energies and volumes of typical composition-conserving defects defined in Sec. II D. These results are presented in Table IV. One can see that all the four sets of results qualitatively agree with each other and predict the same ascending order of the formation energies and very similar formation volumes of the composition-conserving defects.

The agreement is very encouraging due to the relatively small values of the defect energies, on one hand, and differences in computational procedures and approaches on the other. This is so, firstly, because of the difference between all-electron and pseudopotential techniques, and, moreover, between *ab initio* and empirical approaches. Secondly, the effects of the local relaxation around defects are neglected in this study, Fu *et al.*[18] neglected the global (volume) relaxation, whereas the atomic positions were fully relaxed in the

TABLE III. Formation energies E_d (eV) and the relative formation volumes Ω_d/Ω_0, of single point defects in NiAl calculated by the LSGF method with multipole corrections with three different sets of parameters as well as estimated from experimental data, Refs. 28,29,63. Standard states are fcc Ni and fcc Al.

Method	E_d				Ω_d/Ω_0			
	Ni_{Al}	V_{Al}	Al_{Ni}	V_{Ni}	Ni_{Al}	V_{Al}	Al_{Ni}	V_{Ni}
LDA, $l_{max}=2$	1.30	2.69	2.64	0.70	0.21	0.89	0.16	0.64
LDA, $l_{max}=3$	1.25	2.20	2.72	0.66	0.21	0.86	0.10	0.62
GGA, $l_{max}=3$	1.13	1.91	2.51	0.62	0.20	0.84	0.13	0.61
Experiment	1.14			0.38	0.20			0.55

first-principles calculations by Meyer and Fähnle and atomistic simulations by Mishin and Farkas.[53] Note also that our calculations as well as the calculations by Meyer and Fähnle[22] have been performed for larger supercells than those by Fu *et al.*[18]

All the theoretical calculations seem to give a somewhat higher formation energy of a triple defect than expected from experimental estimates.[63,79] On the other hand, the agreement between theoretical and experimental formation volumes of a triple defect is excellent.

The formation energies and volumes of the interbranch defects are also listed in Table IV. The formation energies of the interbranch defects are found to be positive and, therefore, the results of the four theoretical calculations are consistent with each other and predict the same defect structure in the maximally ordered state: antisite Ni atoms for Ni-rich compositions and Ni vacancies for Al-rich compositions.

B. The effect of pressure

A knowledge of the defect formation volumes allows for an analysis of the possible effect of pressure on the defect structure. Since a Ni vacancy has a relatively large formation volume, it is expected that at sufficiently high pressures all constitutional vacancies will be ''pressed out'' and Al-rich NiAl will become a substitutional alloy with only antisite Al atoms present in the ground state. Indeed, since the formation volume of the interbranch Al defect is negative, the enthalpy of this defect must change sign at a pressure of about $p_c \approx 160$ Kbar. Direct calculations of the defect formation enthalpies, i.e., without linearization of Eq. (13), yield a similar result for the crossover pressure, $p_c = 175$ Kbar. However, since the formation enthalpy $H_{V_{Ni}}$ grows very rapidly with pressure, at pressures above 41 Kbar it becomes larger than the formation enthalpy of the stoichiometric NiAl, so the vacancy branch becomes absolutely unstable against a decomposition into pure fcc Al and stoichiometric NiAl at $T=0$.

These results have been basically confirmed by independent pseudopotential calculations,[80] in which both local and global relaxation have been taken into account. In addition, it is found that substitutional solid solution in Al-rich NiAl alloys can be stabilized by further increasing of pressure above 250 Kbar at least with respect to the decomposition into NiAl+fcc Al or NiAl+Ni_2Al_3 two-phase mixtures. Note also, that the mentioned change of the solid solution type in Al-rich NiAl with pressure is predicted to give rise to the first-order phase transition terminated with a critical point.[81] Experimentally, the effect of partial filling of Ni vacancies by Al atoms has been observed in Al-rich alloys at high temperatures under pressures up to 70 Kbar.[82]

C. Defect interactions

The results of our calculations of the defect interaction energies are summarized in Table V. The accuracy of the calculated defect interaction energies is determined by the residual interactions of the two defects at the maximal separation distance within a 108-atom supercell, as well as by the neglect of local relaxation. As follows from our convergence

TABLE IV. Calculated and experimental formation energies, E_{CD} (eV), and relative formation volumes Ω_{CD}/Ω_0 of typical composition-conserving defects in NiAl.

Name	E_{CD}					Ω_{CD}/Ω_0		
	PP[a]	EAM[b]	PP[c]	LSGF[d]	Exp.	PP[c]	LSGF[d]	Exp.
Triple (TN)	2.83	2.05	2.22	2.36	1.90[e] 1.64−1.83[g]	1.19	1.41	1.31[f]
Divacancy (D)	3.07	2.46	2.71	2.53		1.26	1.45	
Exchange (X)	3.15	2.54	3.10	3.63		0.29	0.33	
Triple Al (TA)	6.46	5.41	6.30	6.32		1.61	1.82	
Interbranch Ni (IN)	3.31	2.87	3.20	2.69		1.32	1.49	
Interbranch Al (IA)	0.32	0.49	0.88	1.28		−0.90	−1.08	

[a]Pseudopotential, Ref. 18.
[b]Embedded atom method, Ref. 53.
[c]Pseudopotential, Ref. 22.
[d]This work.
[e]From the enthalpy of alloy formation, Ref. 63.
[f]From the lattice parameter data, Refs. 28,29.
[g]Perturbed angular correlation of gamma rays, Ref. 79.

TABLE V. Interaction energies $E^{\mathrm{int}}_{A-B,n}$ (eV), of various defect pairs in NiAl obtained by the EAM method (Ref. 53) and by the LSGF method (this work) at the calculated equilibrium lattice parameters a_0 of the perfect stoichiometric NiAl.

Defect pair	Coord. shell, n	Distance	EAM	LSGF
$Ni_{Al}-Al_{Ni}$	1	$\frac{1}{2}a_0\langle 111\rangle$	−0.487	−0.557
$V_{Al}-Al_{Ni}$			−0.655	−0.540
$Ni_{Al}-V_{Ni}$			−0.013	0.009
$V_{Al}-V_{Ni}$			0.060	−0.067
$Ni_{Al}-Ni_{Al}$	2	$a_0\langle 100\rangle$	0.185	0.117
$Ni_{Al}-V_{Al}$			0.105	0.126
$V_{Al}-V_{Al}$			−0.081	0.044
$Al_{Ni}-Al_{Ni}$			−0.692	0.103
$Al_{Ni}-V_{Ni}$			0.255	0.063
$V_{Ni}-V_{Ni}$			−0.104	0.126
$Ni_{Al}-Ni_{Al}$	3	$a_0\langle 110\rangle$		−0.001
$V_{Ni}-V_{Ni}$				0.004
$Ni_{Al}-Ni_{Al}$	5	$a_0\langle 111\rangle$		0.012
$V_{Ni}-V_{Ni}$				0.010
$Ni_{Al}-Ni_{Al}$	6	$a_0\langle 200\rangle$		−0.003
$V_{Ni}-V_{Ni}$				0.016

tests, the former contribution is less than 0.01 eV. The contribution due to local relaxations is difficult to estimate without performing the corresponding calculations which are problematic within the ASA. Typical values of the local relaxation energy for isolated point defects in NiAl are of the order of 0.05–0.5 eV (Refs. 21,83) which are comparable with the calculated values of the interaction energy at the first and second coordination shell. However, it is natural to expect that the energy of local relaxation around a defect pair and the energy of local relaxation around isolated defects are of the same order and, therefore, must cancel each other to a large extent when one calculates the defect-defect interaction energy. Thus, one can expect the residual contribution to be only a fraction of the local relaxation energies for isolated defects. Certainly, a direct investigation of this problem would be of great interest.

Let us now analyze what influence the calculated defect interactions might have on the ground-state structure of NiAl. There may be at least two mechanisms by which defect interactions can change the ground state.

(i) Because of the interaction between defects of the same kind, the concentration dependence of the alloy formation energy may become non-linear, so the two branches of alloys (see Fig. 4) may interchange or cross each other at some point,

(ii) Antisite defects and vacancies, all situated on the same sublattice, form bound complexes because of an attractive interaction between them. In this case the two branches of alloys will be ''glued'' together.

We find that the interaction energy of any two defects situated on the same sublattice and separated by a distance of one lattice parameter a_0, is always repulsive and an order of magnitude smaller than the energies of interbranch defects (see Table IV). This means that neither of the two possible mechanisms discussed above can work in NiAl, and the constitution of the ground state obtained for non-interacting defects, Eq. (26), holds.

However, the repulsive character of the interaction between constitutional defects at the shortest possible distance means that in the ground state these defects must form an ordered structure in which they are separated by a distance larger than the lattice parameter a_0. This conclusion is in agreement with the experimentally observed strong tendency of constitutional defects in NiAl to avoid the same kind of defect at the first neighbor distance of their sublattice.[2] In order to determine what kind of ordered structure the constitutional defects form in NiAl, additional information regarding the defects interactions at longer distances is necessary. As Table V shows, $Ni_{Al}-Ni_{Al}$ and $V_{Ni}-V_{Ni}$ interactions beyond the second coordination shell are already very weak. Accordingly, since constitutional defects in NiAl do not have a strong negative interaction energy at any distance, the tendency towards long-range ordering is also weak. This is probably the main reason why mostly short-range order of constitutional defects in NiAl is seen in experiments.[2]

It is noteworthy that the interaction energy of two Ni vacancies has a local minimum at the third coordination shell, which corresponds to the separation distance $a_0\langle 110\rangle$ between the vacancies. This minimum accounts for the structure of the low-temperature Ni_2Al_3 phase, which may be viewed as a continuation of the B2 NiAl phase in which all Ni vacancies are separated by the distance $a_0\langle 110\rangle_{B2}$ in the $\{111\}_{B2}$ plane so that each third $\{111\}_{B2}$ plane of Ni atoms is missing.[28,29] As the separation between vacancies in the $\langle 111\rangle$ direction is $a_0\langle 111\rangle_{B2}$, the resulting rhombohedral structure is additionally stabilized by the relaxation of the c/a ratio. The recently observed Ni_3Al_4 (Ni_3Ga_4 prototype) phase contains constitutional vacancies separated by the $a_0\langle 110\rangle_{B2}$ and $a_0\langle 210\rangle_{B2}$ distances.[47] An intermediate (between short-range and long-range) order of vacancies was observed in Al-rich $B2$ NiAl by electron diffraction.[46] Ni vacancies were found to form characteristic clusters in the $\{111\}$ plane, in which they were separated at a distance of $a_0\langle 110\rangle$.

On the other hand, the structure of the low-temperature Ni-rich phase Ni_5Al_3 (structure type Ga_3Pt_5) can be viewed as a result of ordering of antisite Ni atoms into collinear chains along the $\langle 110\rangle_{B2}$ direction. The chains are separated by distances $a_0\langle 111\rangle_{B2}$ and $a_0\langle 200\rangle_{B2}$, so that two antisite Ni atoms never occur at $a_0\langle 100\rangle_{B2}$ distance from one another. This kind of ordering is consistent with the calculated maximum of the interaction energy within a $Ni_{Al}-Ni_{Al}$ defect pair at a $a_0\langle 100\rangle_{B2}$ distance, as well as with a very shallow pair interaction potential between antisite Ni atoms at longer distances. In the crystal structure proposed for a pre-Martensitic partially ordered Ni-rich NiAl,[41] each antisite Ni atom may have at maximum two $a_0\langle 100\rangle$, four $a_0\langle 110\rangle$, four $a_0\langle 200\rangle$, and eight $a_0\langle 111\rangle$ other antisite Ni neighbors. Our results for the interaction energies strongly suggest that at least $a_0\langle 100\rangle$ neighboring should not occur in the structure, which reduces the maximal possible number of $a_0\langle 111\rangle$ neighbors to four and makes the structure equivalent to the structure of the Ni_5Al_3 phase.

In summary, our calculations show that the onset of defect interactions at low temperatures does not affect the statistics of the constitutional defects in NiAl but leads to a defect ordering which is, in general, consistent with experimental observations.

In Table V we also list the defect interaction energies obtained by Mishin and Farkas.[53] The agreement between the values in the first part of the table is surprising in view of the abovementioned difference in methodology, but so is the disagreement in the second part of the table. The most striking difference exists for an $Al_{Ni}-Al_{Ni}$ defect pair: in our calculations two neighboring antisite Al defects weakly repel each other, whereas in the EAM calculations a strong attractive interaction is obtained the absolute value of which is even larger than the EAM energy of an interbranch Al defect. This means that the EAM calculations actually predict the maximally ordered state of Al-rich alloys to be formed by clusters of antisite Al atoms, whereas Ni vacancies may appear only as thermal defects, in contrast to experimental observations.

The reason for this discrepancy might originate from the internal limitations of the EAM model, which reveal themselves for such a delicate characteristic as the energy of defect-defect interaction. The error due to the neglect of the local relaxation in our calculations cannot be completely excluded either. However, due to the abovementioned effect of cancellation of the local relaxation contributions, the latter error should be too small to cover the whole difference between the calculated $Al_{Ni}-Al_{Ni}$ interaction energies.

V. DEFECTS AT FINITE TEMPERATURES

In this section we present the results of our calculations of the equilibrium defect concentrations in NiAl alloys at 1300 K obtained by numerical solution of Eq. (15). We show that the thermal defect statistics may be interpreted in terms of composition-conserving defects in almost the entire compositional interval. The calculations were performed for noninteracting defects. Possible influence of the defect interactions is briefly discussed at the end of the section.

A. Characterization of thermal defects

The calculated equilibrium atomic concentrations of defects, x_d, in NiAl at 1300 K and zero external pressure are shown in Fig. 5(a) as a function of deviation from stoichiometry δ. The main defects in Ni-rich NiAl are antisite Ni atoms, and in Al-rich NiAl vacancies on the Ni sublattice. Most of these are constitutional defects, the atomic concentrations of which are given by Eq. (26). In this respect, it is useful to separate thermal defects, which appear at a finite temperature, from constitutional defects which are present in the ground state at $T=0$. The concentrations of thermal defects x_d^t in NiAl at 1300 K are plotted in Fig. 5(b).

It is commonly believed that triple defect is the main thermal excitation in NiAl. Indeed, for Ni-rich and stoichiometric NiAl, we find that the dominant thermal defects are vacancies on the Ni sublattice and antisite Ni atoms, which are the constituents of a triple defect. The concentrations of these defects behave as $|\delta|^{-1/2}$ in Ni-rich alloys, in accordance with Eq. (29), whereas the thermal defect concentrations form a sharp peak in the vicinity of the stoichiometric composition, as expected from Eqs. (27) and (28).

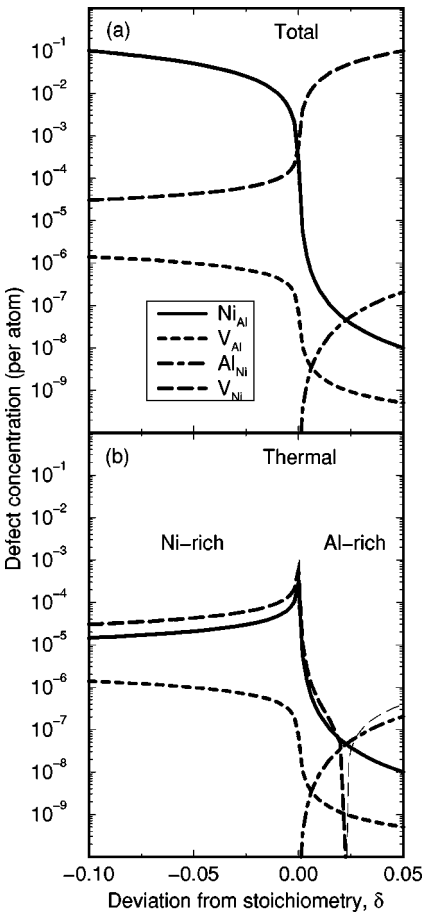

FIG. 5. Equilibrium concentrations of single point defects in $Ni_{1/2-\delta}Al_{1/2+\delta}$ at 1300 K as a function of the deviation from stoichiometry δ: (a) Total defect concentrations; (b) concentrations of thermal defects (defined in the text). The legend in the figure applies to both panels. The thin long-dashed line in panel (b) shows the negative concentration of thermal vacancies on the Ni sublattice.

On the Al-rich side, the concentration of thermal antisite Ni atoms quickly becomes very small with increasing off-stoichiometry, but antisite Al atoms appear in a relatively large amount. These findings are in good agreement with formulas (30) and (31), respectively. The concentration of vacancies on the Ni sublattice behaves even more interestingly. It decreases very rapidly with deviation from stoichiometry, and when the parameter δ exceeds the value of 0.023, the concentration of thermally formed Ni vacancies becomes *negative*. This means that at 1300 K the equilibrium concentration of Ni vacancies in Al-rich NiAl alloys with more than 52.3 at. % Al decreases with temperature. It has been shown in our previous work[84] and independently by Meyer and Fähnle[22] that this kind of thermal behavior can be associated only with the interbranch Al defect, in which two constitutional Ni vacancies are replaced by one antisite Al atom (see Fig. 3).

Let us now demonstrate that the triple defect is the dominant thermal defect in the Ni-rich and stoichiometric NiAl, whereas the interbranch Al defect is the dominant thermal

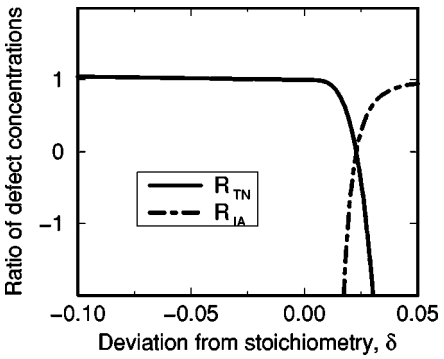

FIG. 6. Ratios of the thermal defect concentrations at 1300 K (see text). R_{TN} is close to one if triple defects dominate in the statistics of thermal defects, R_{IA} is close to one if the dominant thermal defects are interbranch Al defects.

defect in the Al-rich NiAl. In Fig. 6 we show the calculated ratios between the thermal defect concentrations

$$R_{\mathrm{TN}}=\frac{x^t_{V_{\mathrm{Ni}}}}{2x^t_{\mathrm{Ni_{Al}}}},$$

$$R_{\mathrm{IA}}=-\frac{x^t_{V_{\mathrm{Ni}}}}{2x^t_{\mathrm{Al_{Ni}}}}. \tag{37}$$

The ratio R_{TN} should be close to one if the dominant thermal excitations are of triple defect type, while R_{IA} should be close to one if the dominant thermal excitations are the interbranch Al defects. Thus, we find that thermal excitations in NiAl at 1300 K are mainly of triple defect type for $\delta<0.023$ and of interbranch Al type for $\delta>0.023$. At the boundary between the two composition regions, where the crossover $x^t_{\mathrm{Ni_{Al}}}=x^t_{\mathrm{Al_{Ni}}}$ occurs, the thermal excitations can be characterized as exchange defects.

While a triple defect produces three point defects in NiAl, thereby increasing the vacancy concentration, an interbranch defect is a composition-conserving defect which brings totally -1 point defect into the system ($\mathrm{Al_{Ni}}-2V_{\mathrm{Ni}}$) and decreases the concentration of vacancies. The latter type of thermal defect is favored by the entropy term: the removal of two vacancies (which are constitutional, i.e., are present in the ground state in relatively large amount) does not reduce the entropy very much, but the creation of a new (with respect to the ground state) antisite Al defect increases entropy. As a result, the total number of point defects (counted with respect to the ideal $B2$ structure) decreases with temperature, but the entropy increases due to the diversification of the defect structure. Thus, while in Al-rich NiAl alloys the deviation from stoichiometry is formed only due to constitutional Ni vacancies at zero temperature, a certain amount of antisite Al atoms may appear as thermal excitations. According to our calculations, the concentration of antisite Al atoms in Al-rich NiAl at 1300 K does not exceed 10^{-6}, whereas their concentration should be much higher (up to 10^{-3}) according to Fu *et al.*[18] The concentration of antisite Al atoms is determined by the formation enthalpy of interbranch Al defect which, as we have shown in Sec. IV B, is sensitive to pressure and, therefore, to the effects of global and local relaxation. However, the results of all *ab initio* studies agree qualitatively on the fact that interbranch Al defects must be the dominant thermal defects in Al-rich NiAl.

The formation enthalpy of an interbranch Al defect may be considerably reduced by applying external pressure as we have shown in Sec. IV B. Accordingly, one may expect a considerable reduction of the vacancy concentration and a corresponding increase of the concentration of antisite Al atoms at high temperature and pressure. This is exactly what was observed in experiment[82] and called ''vacancy filling.''

Note that a similar ''negative'' behavior of defect concentrations has been reported by Mayer *et al.*[58] for Al-rich FeAl alloys. In that case the situation is completely reversed: the concentration of antisite Al atoms decreases with increasing temperature at the expense of the concentration of vacancies on the Fe sublattice. At high temperatures the latter defects become dominant, whereas at low temperatures Al antisite defects are more stable. This effect can simply be described by the defect reaction $\mathrm{Al_{Fe}}\rightarrow 2V_{\mathrm{Fe}}$, i.e., as an interbranch defect. Due to the low energy of this defect, the number of thermal vacancies becomes so high at elevated temperatures that most of the antisite aluminum atoms on the iron sublattice turn out to be used up. Recent neutron diffraction studies of FeAl performed by Kogachi *et al.*[85,86] seem to confirm this result.

Another example is the defect structure in PdAl which has been calculated by Fu.[19] It can be interpreted as interbranch defects dominating the Al-rich as well as the Pd-rich regions, whereas triple defects dominate only in nearly stoichiometric PdAl. Thus, we see that interbranch defects are rather common thermal defects in off-stoichiometric $B2$ transition-metal aluminides, and must find their place in the list of composition-conserving defects side by side with triple defects.

B. Minimum of the vacancy concentration

At low temperatures, triple defects dominate for the stoichiometric and Ni-rich compositions, whereas interbranch defects become dominant for the Al-rich compositions. Our calculations show that the region in which triple defects dominate expands towards Al-rich compositions with increasing temperature as shown in Fig. 7.

The boundary between the region in which triple defects dominate and the region in which interbranch Al defects dominate can be defined by the crossover condition $x_{\mathrm{TN}}=x_{\mathrm{IA}}$. The crossover concentration δ_B can be estimated from Eqs. (30) and (31):

$$\delta_B\approx\frac{1}{4}\exp[(H_{\mathrm{IA}}-H_{\mathrm{TN}})/4T]. \tag{38}$$

Thus, for an Al-rich alloy (shown in Fig. 7 by a vertical dot-dashed line) the equilibrium vacancy concentration decreases only up to a certain temperature, below which the interbranch Al defects dominate over the triple defect, while above that temperature the vacancy concentration starts to increase because the triple defects become dominant for this alloy composition. As a result, a minimum appears in the temperature dependence of the equilibrium vacancy concentration, as predicted by Smirnov.[34,35] The calculated temperature of the minimum is shown in Fig. 7 by a dashed line.

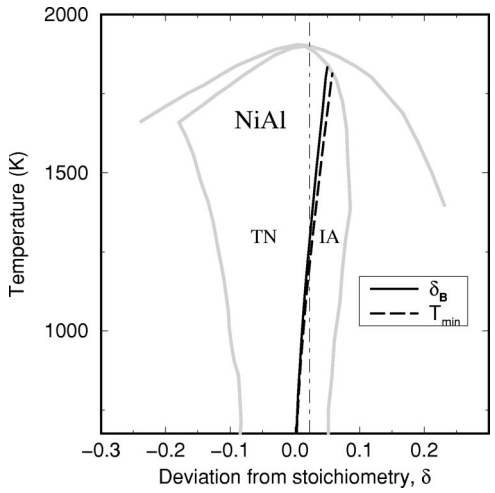

FIG. 7. Boundary between two regions of NiAl in which triple defects (TN) or interbranch Al defects (IA) dominate, respectively (solid line). Temperature at which the equilibrium vacancy concentration takes a minimum (dashed line). Shaded lines depict the phase boundaries of NiAl according to the phase diagram (Ref. 48). Vertical dot-dashed line corresponds to an alloy with a fixed composition ($\delta=0.023$).

The temperature of the minimum $T_{\min}$ for an Al-rich alloy can easily be estimated from the condition $dx_{V_{\mathrm{Ni}}}/dT=0$:

$$\delta\approx\frac{1}{4}\left(\frac{H_{\mathrm{TN}}}{H_{\mathrm{IA}}}\right)^{1/4}\exp[(H_{\mathrm{IA}}-H_{\mathrm{TN}})/4T_{\min}]. \qquad (39)$$

C. Effective vacancy formation energy

The effective formation energies and volumes of single point defects can be calculated using Table I and the numerical values given in Table IV. Moreover, since the dominant thermal defects in all compositional regions of NiAl have been characterized, it is now possible to assign a certain effective formation enthalpy to *thermal* antisite Ni atoms in Ni-rich alloys as well as to *thermal* Ni vacancies in Al-rich region.

Let us concentrate on the effective vacancy formation energy in NiAl, which is mostly determined by thermal Ni vacancies. According to our theoretical calculations, it is equal to $E_V^{\mathrm{eff}}=E_{\mathrm{TN}}/2$ in Ni-rich alloys and $E_V^{\mathrm{eff}}=E_{\mathrm{TN}}/3$ in stoichiometric NiAl. The corresponding numerical estimates may be obtained using the theoretical or experimental values of E_{TN} given in Table IV. For Ni-rich alloys whose composition is close to stoichiometry a crossover behavior for the effective vacancy formation energy is expected between a value of $E_{\mathrm{TN}}/2$ at low temperatures and a value of $E_{\mathrm{TN}}/3$ at high temperatures.

As follows from our calculations, the total concentration of Ni vacancies should decrease in Al-rich alloys at temperatures below $T_{\min}$. In this domain of compositions and temperatures, the formation energy of an interbranch Al defect, E_{IA}, may be regarded as an effective energy of vacancy *annihilation*. At temperatures above the $T_{\min}$ new, thermal Ni vacancies will be created with the effective formation energy $E_V^{\mathrm{eff}}=E_{\mathrm{TN}}$. This complicated behavior of the effective formation energy of thermal vacancies in NiAl as a function of composition and temperature may partly account for the considerable scatter of the experimental data which can be found in the literature.[1,2,52,66,79,87]

D. Thermal defect complexes

Let us now analyze the possible effects of defect interactions on the structure of thermal defects in NiAl. First of all, the fact that the calculated interactions for the $V_{\mathrm{Ni}}-V_{\mathrm{Ni}}$, $V_{\mathrm{Ni}}-\mathrm{Ni}_{\mathrm{Al}}$, and $\mathrm{Ni}_{\mathrm{Al}}-\mathrm{Ni}_{\mathrm{Al}}$ defect pairs are found to be weak and mostly repulsive (see Table V), supports the existing point of view[1] that all three constituents of a triple defect (two vacancies and one antisite defect) exist individually in NiAl without forming a bound complex.

The interactions of point defects separated by the shortest interatomic distance $\frac{1}{2}a_0\langle 111\rangle$ are found to be strong and attractive in two cases. Our calculations give a large negative interaction energy between the constituents of an exchange defect, therefore, the exchange pair $\mathrm{Ni}_{\mathrm{Al}}-\mathrm{Al}_{\mathrm{Ni}}$ should exist as a bound complex in NiAl. The lowering of the formation energy of the exchange pair due to the interaction between $\mathrm{Ni}_{\mathrm{Al}}$ and $\mathrm{Al}_{\mathrm{Ni}}$ is still insufficient to make exchange pairs the dominant thermal defects in Al-rich NiAl alloys.

A large attractive interaction is also found between an antisite Al atom and a vacancy on the Al sublattice. However, due to the large formation enthalpy of the triple Al defect (Table IV) it seems unlikely that the influence of the defect interaction on the equilibrium defect concentrations would be significant.

However, the first-neighbor defect pairs discussed above may be formed in the course of atomic diffusion as a result of subsequent vacancy jumps.[88–91] Their formation and interaction energies are therefore valuable for understanding the kinetic processes in NiAl.

The physical reason for the strong attractive $\mathrm{Ni}_{\mathrm{Al}}-\mathrm{Al}_{\mathrm{Ni}}$ and $\mathrm{Al}_{\mathrm{Ni}}-V_{\mathrm{Al}}$ interactions is the reduction of the number of energetically unfavorable Al-Al bonds, which are replaced by strong Ni−Al bonds upon the formation of the defect complexes. A very rough estimate of the pair interaction energies within this simplest nearest-neighbor bond picture $E^{\mathrm{int}}\approx\frac{1}{2}\Delta H_{\mathrm{NiAl}}$, agrees well with the results of rigorous calculations. Another contribution is due to a reduction of the elastic energy within the defect complexes.

VI. SUMMARY

The formation enthalpies of point defects in NiAl as well as the interaction energies of various defect pairs have been calculated by an order-N, locally self-consistent Green's-function method within the ASA+M approach. We have found that the ground state of off-stoichiometric NiAl alloys is formed by antisite Ni atoms on the Al sublattice in Ni-rich NiAl and by vacancies on the Ni sublattice in Al-rich NiAl. According to the calculated defect interactions, the constitutional defects of the same kind must form ordered structures in the ground state, in which they tend to avoid each other at the shortest possible distance on their sublattice.

The equilibrium defect concentrations at finite temperatures are studied both numerically and analytically within the Wagner-Schottky model using a canonical ensemble. The

dominant point defects are characterized and their effective formation energies are obtained for the stoichiometric as well as for the off-stoichiometric alloy compositions.

The dominant thermal defects are shown to be triple defects in Ni-rich and stoichiometric NiAl and interbranch Al defects in Al-rich NiAl. Since an interbranch Al defect annihilates two constitutional vacancies and creates only one antisite Al atom, the equilibrium amount of vacancies as well as the total number of point defects must *decrease* with temperature in Al-rich NiAl at low temperatures.

The calculated defect interactions indicate that all three constituents of a triple defect may exist individually in NiAl without forming a bound complex. In contrast, a strong attractive interaction was found for the following defect pairs in NiAl: Ni on the Al sublattice and Al on the Ni sublattice, and vacancy on the Al sublattice and Al on the Ni sublattice. Although the defect interactions are shown to have only minor effects on the equilibrium defect concentrations, they may be of importance for understanding the kinetic processes and metastable defect arrangements in NiAl.

ACKNOWLEDGMENTS

The authors wish to express their gratitude to H. L. Skriver and Y. M. Mishin for carefully reading the manuscript and making many helpful remarks. P.K. and A.L. are indebted to M. W. Finnis and P. Gumbsch for valuable discussions and comments. We are grateful to M. Fähnle for making the results of Ref. 22 available to us prior to publication. This work was partially financed by SKB AB, the Swedish Nuclear Fuel and Waste Management Company. Support by the Swedish Natural Science Research Council and the Swedish Materials Consortium No. 9 is acknowledged. I.A.A. is grateful to the Swedish Foundation for Strategic Research for financial support. The Center for Atomic-Scale Materials Physics is sponsored by the Danish National Research Foundation. Support by the Russian Foundation for Basic Research is acknowledged by P.K., A.L., and Y.V. (Grants No. 97-02-17261 and No. 98-02-16419).

[1] D.B. Miracle, Acta Metall. Mater. **41**, 649 (1993).
[2] R.D. Noebe, R.R. Bowman, and M.V. Nathal, Int. Mater. Rev. **38**, 193 (1993).
[3] A.E. Carlsson, Phys. Rev. B **40**, 912 (1989).
[4] T. Hong and A.J. Freeman, Phys. Rev. B **43**, 6446 (1991).
[5] Z.W. Lu, S.-H. Wei, and A. Zunger, Acta Metall. Mater. **40**, 2155 (1992).
[6] J.A. Moriarty and M. Widom, Phys. Rev. B **56**, 7905 (1997).
[7] D. Hackenbracht and J. Kübler, J. Phys. F **10**, 427 (1980).
[8] J.M. Koch and C. Koenig, Philos. Mag. B **54**, 177 (1986); **55**, 359 (1987); **57**, 557 (1988).
[9] P.A. Schultz and J.W. Davenport, J. Alloys Compd. **197**, 229 (1993).
[10] J. Zou and C.L. Fu, Phys. Rev. B **51**, 2115 (1995).
[11] G.A. Botton, G.Y. Guo, W.M. Temmerman, and C.J. Humphreys, Phys. Rev. B **54**, 1682 (1996).
[12] D.A. Muller, D.J. Singh, and J. Silcox, Phys. Rev. B **57**, 8181 (1998).
[13] Z.W. Lu, S.-H. Wei, A. Zunger, S. Frota-Pessoa, and L.G. Ferreira, Phys. Rev. B **44**, 512 (1991).
[14] B.P. Burton, J.E. Osburn, and A. Pasturel, Phys. Rev. B **45**, 7677 (1992).
[15] A. Pasturel, C. Colinet, A.T. Paxton, and M. van Schilfgaarde, J. Phys.: Condens. Matter **4**, 945 (1992).
[16] M. J. Mehl, B. M. Klein, and D. A. Papaconstantopoulos, in *Intermetallic Compounds:* Vol. 1, *Principles*, edited by J.H. Westbrook and R.L. Fisher (Wiley, New York, 1994), p. 195.
[17] K. Rzyman, Z. Moser, R.E. Watson, and M. Weinert, J. Phase Equilib. **19**, 106 (1998).
[18] C.L. Fu, Y.-Y. Ye, M.H. Yoo, and K.M. Ho, Phys. Rev. B **48**, 6712 (1993).
[19] C.L. Fu, Phys. Rev. B **52**, 3151 (1995).
[20] N.I. Medvedeva, O.N. Mryasov, Yu.N. Gornostyrev, D.L. Novikov, and A.J. Freeman, Phys. Rev. B **54**, 13 506 (1996).
[21] N.I. Medvedeva, Yu.N. Gornostyrev, D.L. Novikov, O.N. Mryasov, and A.J. Freeman, Acta Mater. **46**, 3433 (1998).
[22] B. Meyer and M. Fähnle, Phys. Rev. B **59**, 6072 (1999); **60**, 717 (1999).
[23] D.J. Peterman, R. Rosei, D.W. Lynch, and V.L. Moruzzi, Phys. Rev. B **21**, 5505 (1980).
[24] V.E. Egorushkin, A.I. Kul'mentyev, and P.E. Rubin, Solid State Commun. **57**, 821 (1986).
[25] D. Knab and C. Koenig, J. Phys.: Condens. Matter **2**, 465 (1990).
[26] K.J. Kim, B.N. Harmon, and D.W. Lynch, Phys. Rev. B **43**, 1948 (1991).
[27] O.V. Farberovich, S.V. Vlasov, K.I. Portnoi, and A.Yu. Lozovoi, Physica B **182**, 267 (1992).
[28] A.J. Bradley and A. Taylor, Proc. R. Soc. London, Ser. A **159**, 56 (1937).
[29] A. Taylor and N.J. Doyle, J. Appl. Crystallogr. **5**, 201 (1972).
[30] S. Konobeevsky, J. Inst. Met. **63**, 161 (1938).
[31] W. Hume-Rothery, J.O. Betterton, and J. Reynolds, J. Inst. Met. **80**, 609 (1952).
[32] H. Jones, *The Theory of Brillouin Zones and Electronic States in Crystals* (North-Holland, Amsterdam, 1960).
[33] H. Lipson and A. Taylor, Proc. R. Soc. London, Ser. A **173**, 232 (1939).
[34] A.A. Smirnov, Dokl. Akad. Nauk (SSSR) **318**, 1166 (1991) [Sov. Phys. Dokl. **36**, 479 (1991)].
[35] A.A. Smirnov, Metallofizika (Kiev) **14**, 3 (1992) [Phys. Metals **12**, 377 (1993)].
[36] A.H. Cottrell, Intermetallics **3**, 341 (1995).
[37] A.H. Cottrell, Intermetallics **5**, 467 (1997).
[38] V.E. Egorushkin, A.I. Kul'mentyev, and P.E. Rubin, Fiz. Met. Metalloved. **60**, 821 (1985).
[39] G.L. Zhao and B.N. Harmon, Phys. Rev. B **45**, 2818 (1992).
[40] G. M. Stocks, W.A. Shelton, D.M. Nicholson, F.J. Pinski, B. Ginatempo, A. Barbieri, B.L. Györffy, D.D. Johnson, J.B. Staunton, P.E.A. Turchi, and M. Sluiter, in *Ordered Intermetallics–Physical Metallurgy and Mechanical Behaviour*, edited by C.T. Liu *et al.* (Elsevier, Amsterdam, 1992), p. 15.
[41] S. Rosen and J.A. Goebel, Trans. Soc. Min. Eng. AIME **242**, 722 (1968).

[42] K. Enami, S. Nenno, and K. Shimizu, Trans. Jpn. Inst. Met. **14**, 161 (1973).
[43] L.E. Tanner, A.R. Pelton, G. van Tendeloo, D. Schryvers, and M.E. Wall, Scr. Metall. Mater. **24**, 1731 (1990).
[44] G.W. West, Philos. Mag. **9**, 979 (1964).
[45] M.J. Cooper, Philos. Mag. **10**, 735 (1964).
[46] R. de Ridder, G. van Tendeloo, and S. Amelinckx, Phys. Status Solidi A **43**, 133 (1977).
[47] M. Ellner, S. Kek, and B. Predel, J. Less-Common Met. **154**, 207 (1989).
[48] P.D. Desai, J. Phys. Chem. Ref. Data **16**, 109 (1987).
[49] A.V. Ruban and H.L. Skriver, Phys. Rev. B **55**, 856 (1997).
[50] R.J. Wasilewski, J. Phys. Chem. Solids **29**, 39 (1968).
[51] S.M. Kim, Phys. Rev. B **33**, 1509 (1986).
[52] K.A. Badura and H.-E. Schaefer, Z. Metallkd. **84**, 405 (1993).
[53] Y. Mishin and D. Farkas, Philos. Mag. A **75**, 169 (1997).
[54] M. W. Finnis, in *Properties of Complex Inorganic Solids*, edited by Gonis *et al.* (Plenum Press, New York, 1997), p. 339.
[55] M. Hagen and M.W. Finnis, Philos. Mag. A **77**, 447 (1998).
[56] C. Wagner and W. Schottky, Z. Phys. Chem. Abt. B **11**, 163 (1930).
[57] S.M. Foiles and M.S. Daw, J. Mater. Res. **2**, 5 (1987).
[58] J. Mayer, C. Elsässer, and M. Fähnle, Phys. Status Solidi B **191**, 283 (1995).
[59] J. Mayer and M. Fähnle, Acta Mater. **45**, 2207 (1997).
[60] V. Schott and M. Fähnle, Phys. Status Solidi B **204**, 617 (1997).
[61] M. Kogachi, Y. Takeda, and T. Tanahashi, Intermetallics **3**, 129 (1995).
[62] In theory of order-disorder transitions in alloys, the long-range order parameters are defined in terms of site concentrations as $\eta_{\mathrm{Ni}}=c_{\mathrm{Ni}_{\mathrm{Ni}}}-c_{\mathrm{Ni}_{\mathrm{Al}}}$ and $\eta_{\mathrm{Al}}=c_{\mathrm{Al}_{\mathrm{Al}}}-c_{\mathrm{Al}_{\mathrm{Ni}}}$. Our definition of the LRO parameters coincides with the usual definition at zero vacancy concentration.
[63] E.-T. Henig and H.L. Lukas, Z. Metallkd. **66**, 98 (1975).
[64] It is the exact result for noninteracting defects that the dominant thermal defect at low temperatures must involve only two types of point defects. In other words, at low temperatures the trajectory of an alloy in the domain of possible alloy configurations goes along an edge of the domain, away from the vortex corresponding to the maximally ordered state, with a possible deviation from this direction at high temperatures. Therefore, the dominant thermal defect can be found by enumerating all the edges of the domain of possible alloy configurations.
[65] M.A. Krivoglaz and A.A. Smirnov, Fiz. Met. Metalloved. **60**, 207 (1985).
[66] H.-E. Schaefer, K. Frenner, and R. Würschum, Phys. Rev. Lett. **82**, 948 (1999).
[67] K. Badura-Gergen and H.-E. Schaefer, Phys. Rev. B **56**, 3032 (1997).
[68] I.A. Abrikosov, A.M.N. Niklasson, S.I. Simak, B. Johansson, A.V. Ruban, and H.L. Skriver, Phys. Rev. Lett. **76**, 4203 (1996).
[69] I.A. Abrikosov, S.I. Simak, B. Johansson, A.V. Ruban, and H.L. Skriver, Phys. Rev. B **56**, 9319 (1997).
[70] T. Beuerle, R. Pawellek, C. Elsässer, and M. Fähnle, J. Phys.: Condens. Matter **3**, 1957 (1991).
[71] P. Braun, M. Fähnle, M. van Schilfgaarde, and O. Jepsen, Phys. Rev. B **44**, 845 (1991).
[72] M. Sinder, D. Fuks, and J. Pelleg, Phys. Rev. B **50**, 2775 (1994).
[73] L. Vitos, J. Kollàr, and H.L. Skriver, Phys. Rev. B **55**, 13 521 (1997).
[74] H.L. Skriver and N.M. Rosengaard, Phys. Rev. B **46**, 7157 (1992).
[75] P.A. Korzhavyi, I.A. Abrikosov, B. Johansson, A.V. Ruban, and H.L. Skriver, Phys. Rev. B **59**, 11 693 (1999).
[76] J.P. Perdew, K. Burke, and M. Ernzerhof, Phys. Rev. Lett. **77**, 3865 (1996).
[77] R.J. Wasilewski, Trans. Soc. Min. Eng. AIME **236**, 455 (1966).
[78] J.W. Otto, J.K. Vassiliou, and G. Frommeyer, J. Mater. Res. **12**, 3106 (1997).
[79] B. Bai and G.S. Collins, in *High-Temperature Ordered Intermetallic Alloys VIII*, MRS Symposia Proceedings No. 552, edited by E.P. George, M. Yamaguchi, and M.J. Mills (Materials Research Society, Pittsburgh, 1999), pp. KK8.7.1-6.
[80] A.Y. Lozovoi, P.A. Korzhavyi, A. Alavi, and M.W. Finnis, Bull. Am. Phys. Soc. **44**, 1855 (1999). The abstract is available at URL http://titus.phy.qub.ac.uk
[81] A. Alavi, A.Y. Lozovoi, and M.W. Finnis, Phys. Rev. Lett. **83**, 979 (1999).
[82] A. Taylor and N.J. Doyle, J. Appl. Crystallogr. **5**, 210 (1972).
[83] A.Y. Lozovoi (unpublished).
[84] P.A. Korzhavyi, I.A. Abrikosov, and B. Johansson, in *High-Temperature Ordered Intermetallic Alloys VIII* (Ref. 79), pp. KK5.35.1-8.
[85] M. Kogachi, T. Haraguchi, and S.M. Kim, Intermetallics **6**, 499 (1998).
[86] T. Haraguchi and M. Kogachi, in *High-Temperature Ordered Intermetallic Alloys VIII* (Ref. 79), pp. KK5.33.1-7.
[87] R. Würschum, K. Badura-Gergen, E.A. Kümmerle, C. Grupp, and H.-E. Schaefer, Phys. Rev. B **54**, 849 (1996).
[88] E.W. Elcock and C.W. McCombie, Phys. Rev. **109**, 605 (1958).
[89] P. Wynblatt, Acta Metall. **15**, 1453 (1967).
[90] A. Bose, G. Frohberg, and H. Wever, Phys. Status Solidi A **52**, 509 (1979).
[91] Y. Mishin and D. Farkas, Philos. Mag. A **75**, 187 (1997).